CHEMISTRY OF MATERIALS

pubs.acs.org/cm

Article

Cr^{2+} in Square Planar Coordination: Durable and Intense Magenta Pigments Inspired by Lunar Mineralogy

Published as part of Chemistry of Materials virtual special issue "C. N. R. Rao at 90".

Anjali Verma, Jun Li, and M. A. Subramanian*

Cite This: https://doi.org/10.1021/acs.chemmater.4c00253

Read Online

ACCESS | Metrics & More | Article Recommendations

ABSTRACT: To date, no terrestrial mineral has been reported to contain Cr^{2+} as one of its major components. However, the occurrence of Cr^{2+} in lunar phases has stimulated interest in investigating the mineral chemistry of inorganic compounds containing the divalent form of chromium. Furthermore, Cr^{2+} is similar to Mn^{3+} (the chromophore responsible for the intense color in YInMn blue ($YIn_{1-x}Mn_xO_3$)), and both are d^4 and exhibit Jahn−Teller distortion, opening up the possibility for Cr^{2+} being a chromophore for designing pigments. Bulk samples of $Ca_{1-x}Mg_xCrSi_4O_{10}$ containing Cr^{2+} were synthesized by high-temperature solid-state reaction methods under reduced oxygen fugacity (under a vacuum and/or N_2/H_2 gas mixture) in search of intense and durable pigments. The polycrystalline phases crystallize in a tetragonal crystal structure (space group: $P4/ncc$) and are isostructural to mineral gillespite ($BaFeSi_4O_{10}$) and Egyptian blue ($CaCuSi_4O_{10}$). Magnetic susceptibility measurements confirmed the presence of chromium in the divalent state. The $Ca_{1-x}Mg_xCrSi_4O_{10}$ (x = 0−0.2) samples exhibit different shades of magenta, varying with Mg content. The optical spectra of the series are consistent with Cr^{2+} (d^4) in square planar coordination with $^5B_{1g}$ as the ground state, corresponding to the configuration $d^1_{z^2}$, $d^2_{xz,\ yz}$, d^1_{xy}, $d^1_{x^2-y^2}$. The observed spectra can be attributed to electronic transitions from the $^5B_{1g}$ state to other quintet states of Cr^{2+}: $^5B_{2g}$, ^5E_g, and $^5A_{1g}$. The origin of the intense magenta color in the solid solutions is ascribed to the synergistic effect of d-d transitions allowed via vibronic coupling through simultaneous excitation of the u vibrational mode of the $[CrO_4]$ unit consisting of A_{2u}, B_{2u}, and E_u symmetries. The formation of intense reddish-magenta pigments with Cr^{2+} in square planar coordination opens the door to exploring novel pigments with divalent chromium in diverse coordination environments.

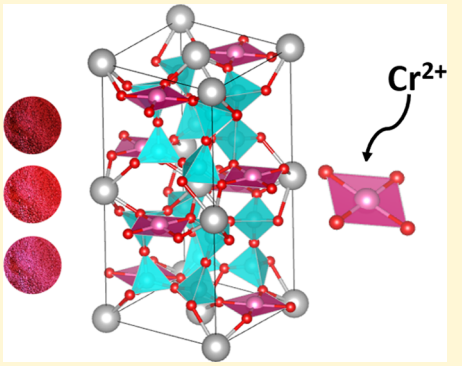

INTRODUCTION

Today, solid-state chemistry is mainly concerned with the new strategies to tailor materials with desired and controllable properties such as electronic, magnetic, dielectric, optical, or catalytic.[1] Among solid-state materials, inorganic transition metal oxides play an important role in the design of functional materials such as inorganic color pigments used in heat-reflecting energy-saving coating applications.[2] Due to a worldwide increase in chemical safety regulations, the colorant industry is in high gear to find replacements for pigments that contain toxic/carcinogenic elements, such as cadmium, lead, mercury, hexavalent chromium, antimony, and cobalt. For example, current commercially available violet/magenta-colored pigments are based on cobalt phosphates (e.g., NH_4CoPO_4, $Co_3(PO_4)_2$) where cobalt is considered as a carcinogen.[2] Given the considerations mentioned above, there is a need to find safer alternatives.

The origin of color in gemstones and minerals has been studied extensively.[3−5] In spite of recent advancements in quantum mechanical theories and computational methods, predicting a crystal lattice that will produce an inorganic pigment with certain intense color is still very difficult.[6,7] Transition metal cations engender color in materials because they have electronic transition energies that match with wavelengths in the visible range (380−720 nm). Among the various electronic transitions, the d-d transition is the most common origin of color in transition metal compounds and minerals.[8] Factors such as the coordination geometry of chromophores and number of unpaired electrons can have a huge influence on the color and intensity of crystal field spectra and are governed by probabilities of electronic transitions between split $3d$ orbital energy levels. The probabilities are normally expressed qualitatively by using selection rules, specifically the spin-multiplicity selection rule (ΔS = 0) and

Received: January 28, 2024
Revised: March 27, 2024
Accepted: March 28, 2024

the orbital (Laporte) selection rule.[9] When an electronic transition takes place via light absorption, the orbital selection rule dictates that there should be a change in the transition dipole moment which can occur only between orbital states that differ in parity ($g \leftrightarrow u$, $\Delta l = \pm 1$, l: azimuthal quantum number).[9] Usually, chromophores at noncentrosymmetric coordination, such as tetrahedral (T_d), trigonal bipyramidal (D_{3h}), and square pyramidal (C_{4v}), are preferred for pigments with intense colors due to relaxation in the orbital selection rule via *d*-orbital/*p*-orbital mixing (hybridization). Such a *d*-*p* mixing is not possible when a chromophore is placed in a crystallographic site with an inversion center such as a perfect octahedron (O_h) or square planar (D_{4h}) coordination.[9]

Egyptian blue, discovered 5000 years ago in Egypt, is a crystalline compound whose composition corresponds to a copper calcium tetrasilicate, $CaCuSi_4O_{10}$.[10−12] Egyptian blue (later found as a rare mineral, cuprorivaite[13]) has a layered structure composed of rings of four SiO_4 tetrahedra $[Si_4O_{10}]^{4-}$ which are linked together by CuO_4 square planar units. It is isostructural to mineral gillespite with a formula $BaFeSi_4O_{10}$, where Fe^{2+} occupies rare square planar coordination (D_{4h}).[14] The observation of blue color in $CaCuSi_4O_{10}$ with Cu^{2+} in centrosymmetric square planar coordination is due to the vibronic coupling, that is, a coupling between *d*-*d* electronic and vibrational wave functions involving asymmetric modes (u), which in turn can relax the orbital selection rule.[15]

In 2009, Subramanian and his co-workers discovered an intense blue pigment with Mn^{3+} in the trigonal bipyramidal sites in a solid solution between hexagonal $YMnO_3$ and $YInO_3$.[16,17] This led us to explore new pigments with divalent chromium as chromophore since Cr^{2+} and Mn^{3+} are isoelectronic (d^4 electron configuration), and both show Jahn−Teller distortions. But, unlike Mn^{3+}, Cr^{2+} is a rare occurrence in terrestrial minerals, gemstones, and synthetic oxides. In 1970, Haggerty et al.[18,19] reported the first observation of Cr^{2+} in lunar minerals and later by Meyer and Boyd[20] as olivine inclusions in terrestrial diamonds from kimberlites. To date, no terrestrial mineral has been reported to contain Cr^{2+} as one of the major components. In 1981, Gasparik[21] attempted to synthesize Cr^{2+}-containing phases in the system, CaO-MgO-Cr^0-Cr_2O_3-SiO_2, by heating the starting mixtures to high temperatures under vacuum. The synthesis yielded small single crystals of unknown compositions. X-ray structure refinements[22] using single crystals picked up from the melt showed the formation of $CaCrSi_4O_{10}$ and found to be an isostructural analogue of the layered silicates $MM'Si_4O_{10}$ (M = Ca, Ba, Sr, and M' = Cu, Fe)[12,14,15] with Cr^{2+} occupying nearly square planar coordination and Si^{4+} and Ca^{2+} occupying tetrahedral and irregular cubic coordination ($\bar{4}$ symmetry), respectively. The projection of the crystal structure is shown in Figure 1. Crystal structure analyses of $CaCrSi_4O_{10}$ single crystals verified a bond valence sum of 1.94 for Cr;[22,23] however, no direct experimental evidence (e.g., magnetic measurements) was given to show that chromium is present in a divalent state in this compound, and no optical properties were reported for polycrystalline samples.

We have investigated the $Ca_{1-x}Mg_xCrSi_4O_{10}$ system with Cr^{2+} in square planar coordination in the search for intense and durable pigments with tunable hues. For the first time, bulk samples of this series of compounds have been prepared and found to give an intense, tunable reddish-magenta color up to $x = 0.2$. The origin of color in these solid solutions is based on the coupling between vibrational and electronic energy levels, and this "vibronic" coupling, in turn, relaxes the orbital selection rule, leading to an intense color.

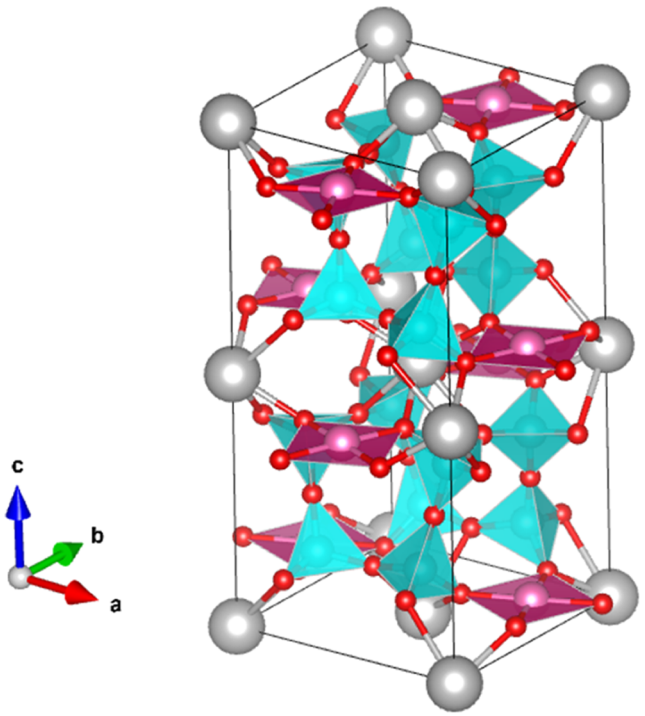

Figure 1. Schematic of the unit cell of $CaCrSi_4O_{10}$ projected along the *c*-axis. Ca and O atoms are shown in gray and red colors, respectively, while Cr and Si are shown as magenta and turquoise polyhedra, respectively.

EXPERIMENTAL SECTION

Polycrystalline samples of $Ca_{1-x}Mg_xCrSi_4O_{10}$ (x = 0−0.2) were prepared through two different solid-state synthesis methods. Stoichiometric amounts of MgO (CERAC, 99.5%), SiO_2 (CERAC, 99.5%), $CaSiO_3$ (BTC, 99%), Cr_2O_3 (Alfa Aesar, 99.98%), and Cr^0 (Alfa Aesar, 99.95%) were ground in an agate mortar, pressed into pellets, and heated between 1350 and 1400 °C for 0.5−1 h in thick-walled (1.5 mm) sealed quartz ampules (99.99% purity quartz tube obtained from GM Quartz, Oakland, CA) under vacuum (10^{-4} mm Hg) and/or under N_2/H_2 (95/5%) atmosphere in a high-temperature tube furnace capable of reaching 1600 °C (Carbolite, UK). To keep the oxygen fugacity low, a very slight excess of Cr metal (0.04 mol) was used. The samples were reground and reheated repeatedly to complete the reaction. All of the samples used in this study were prepared under a N_2/H_2 atmosphere to avoid trace contamination from the quartz ampule, if any.

Phase purity and unit cell parameters were determined using powder X-ray diffraction (XRD) on a benchtop Rigaku Miniflex II powder diffractometer with Cu Kα radiation and a graphite monochromator. Lattice parameters were refined by LeBail fit using GSAS EXPGUI software and KCl ($Fm\bar{3}m$) as an internal standard. Magnetic measurements (10−350 K) were obtained using a Quantum Design MPMS. NIR reflectance measurements were performed using a Jasco V-670 spectrometer with the Spectralon (fluoropolymer) as the white standard up to 2500 nm and converted to absorbance using the Kubelka−Munk equation. Color coordinates in the CIELAB color space were measured using a Konica Minolta CM-700d spectrophotometer with daylight as the illumination source. Thermogravimetric analysis (TGA) was performed using a TA Instruments Model TGA Q50. The weight loss or weight gain was assessed upon heating the samples under air flow to 800 °C with a ramp rate of 5 °C/min. Samples of $CaCrSi_4O_{10}$ were stirred in 50% HNO_3 (aq.) and 1 M

https://doi.org/10.1021/acs.chemmater.4c00253
Chem. Mater. XXXX, XXX, XXX−XXX

NaOH for 8 h and filtered, and their color properties and phase purity were determined via XRD to determine acid and base resistance.

RESULTS AND DISCUSSION

Powder X-ray diffraction data of the $Ca_{1-x}Mg_xCrSi_4O_{10}$ (x = 0−0.2) series are shown in Figure 2. XRD patterns of all pure

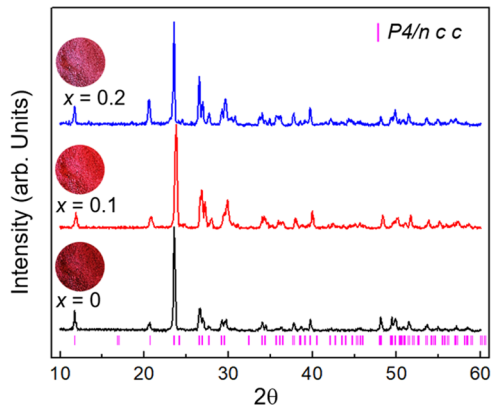

Figure 2. X-ray diffraction patterns and sample images of the $Ca_{1-x}Mg_xCrSi_4O_{10}$ (x = 0−0.2) series. The vertical bars (pink) indicate the expected reflection positions for the tetragonal ($P4/ncc$) phases.

samples can be indexed well in the tetragonal space group $P4/ncc$. The samples show different shades of magenta. LeBail fit for the $CaCrSi_4O_{10}$ sample is shown in Figure 3. The

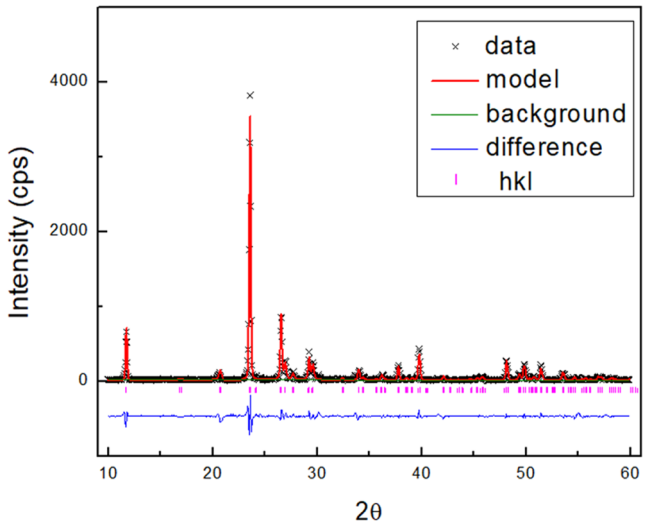

Figure 3. LeBail refinement of $CaCrSi_4O_{10}$. The vertical bars (pink) indicate the expected reflection positions for the tetragonal ($P4/ncc$) phases.

maximum miscibility limit of magnesium is found to be x = 0.2, after which the X-ray patterns begin to show the unreacted starting materials. The addition of Mg^{2+} decreases the unit cell parameters due to the smaller size of Mg^{2+} relative to Ca^{2+} (Table 1).[24]

The Ca ions are slightly underbonded in the distorted cubic coordination and the tetragonal cell volume of $CaCrSi_4O_{10}$ can be compressed by 4.6% under high pressures.[22] The solubility limit of Mg in this flexible framework is presumably due to the reluctance of Mg^{2+} to adopt a coordination number higher

Table 1. Lattice Parameters for the $Ca_{1-x}Mg_xCrSi_4O_{10}$ (x = 0−0.2) Series

composition	a or b (Å)	c (Å)
$CaCrSi_4O_{10}$	7.375 (1)	15.110 (1)
$Ca_{0.9}Mg_{0.1}CrSi_4O_{10}$	7.365 (2)	15.100 (1)
$Ca_{0.8}Mg_{0.2}CrSi_4O_{10}$	7.363 (1)	15.098 (3)

than six. The small variation of magenta color upon Mg substitution can be ascribed to the rigidity of the four Cr−O bonds[23] in the square planar CrO_4 groups that prevents the modification of the local environment around Cr^{2+} chromophores.

Magnetic measurement was performed for the $CaCrSi_4O_{10}$ sample to verify the oxidation state of the chromium ion. Temperature dependence of the magnetic susceptibility (χ) is given in Figure 4 (left). Using the slope and intercept obtained by fitting the high-temperature linear region (150−350 K) of inverse magnetic susceptibility ($1/\chi$) vs temperature plot (Figure 4 (right)), Curie constants (C) and Weiss constants (θ_W) were determined. Effective magnetic moments (μ_{eff}) were calculated from Curie constants with diamagnetic correction.[25] The studied compounds show paramagnetic behavior in the measured temperature range of 10−350 K. The calculated effective magnetic moment values are comparable to the theoretical spin-only magnetic moments for high spin Cr^{2+} ($3d^4$, μ_{th} = 4.89 μB, μ_{exp} = 4.80 μB) in $CaCrSi_4O_{10}$. The existence of divalent chromium is confirmed experimentally.

Thermogravimetric analysis (TGA) after heating the $CaCrSi_4O_{10}$ sample under air flow to 800 °C shows that the compound is fairly stable up to 500 °C, followed by a color change and a slight weight gain of nearly 0.59(1)% (Figure 5). XRD analysis of the TGA residue still shows the presence of the tetragonal ($P4/ncc$) phase with a negligible change in lattice parameters (Figure 6). XRD analysis, weight gain, and color change collectively led us to conclude the presence of a very small amount of excess oxygen in the same structure ($P4/ncc$) with the formula $CaCrSi4O_{10.14}$ containing Cr^{3+}. Close examination of the crystal structure reveals that there are available crystallographic sites to accommodate excess oxygen above and below the planar [CrO_4] unit. When the $CaCrSi_4O_{10}$ sample was heated at 1000 °C in air for 12 h, it changed to a green color, and the XRD analysis of the sample revealed the complete decomposition of the compound with the formation of Cr_2O_3 (Figure 6).

The color of these materials has been evaluated using the CIE $L^*a^*b^*$ color space. It is a three-dimensional color model where $L^*a^*b^*$ uses three primary numbers to quantify the brightness (L^*), green-red (a^*), and blue-yellow (b^*) values. Higher L^* values are the result of brighter colors with a higher light reflectivity. Positive a^* values correspond to more red coloration, while more negative b^* values are more blue.[26] The $L^*a^*b^*$ color coordinates for $Ca_{1-x}Mg_xCrSi_4O_{10}$ (x = 0−0.2) magenta pigments with tunable hues are mentioned in Table 2.[27,28]

To check the stability and durability of $Ca_{1-x}Mg_xCrSi_4O_{10}$ magenta pigments under rigid acidic and basic conditions, a series of experiments were performed. Specimens of $CaCrSi_4O_{10}$ were stirred in either 50% HNO_3 (aq.) or 1 M NaOH for 8h, filtered, and examined via $L^*a^*b^*$ color measurements and X-ray diffraction. XRD patterns (Figure 7) show no noticeable change in the crystal structure, and $L^*a^*b^*$ measurements reveal no change in color. This is consistent

https://doi.org/10.1021/acs.chemmater.4c00253
Chem. Mater. XXXX, XXX, XXX−XXX

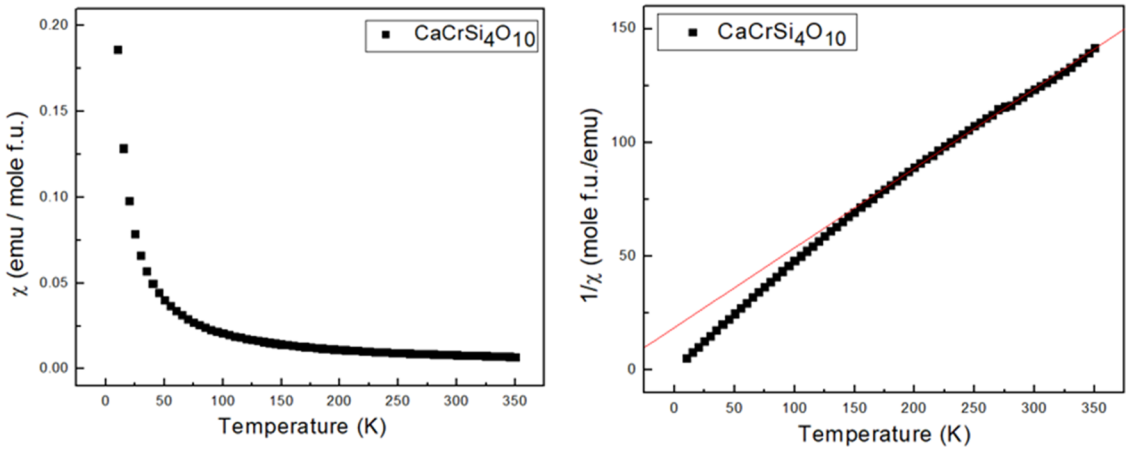

Figure 4. Magnetic susceptibility (left) and Inverse magnetic susceptibility (right) of $CaCrSi_4O_{10}$ as a function of temperature. 1 emu (cgs units) = 10^{-3} A m^2 (SI units).

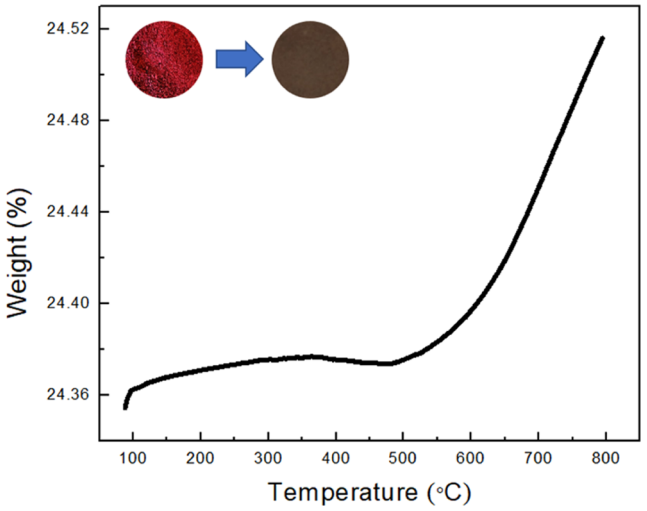

Figure 5. TGA in air for a $CaCrSi_4O_{10}$ sample.

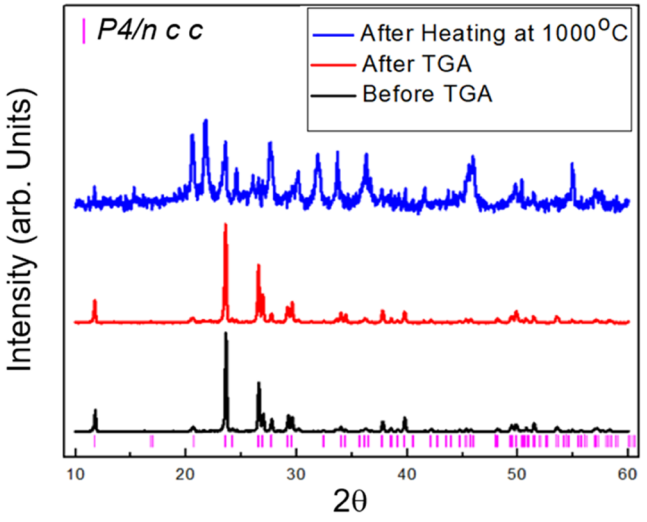

Figure 6. XRD patterns of $CaCrSi_4O_{10}$ samples after heating at 1000 °C in air and before/after TGA (800 °C in air flow). The vertical bars (pink) indicate the expected reflection positions for the tetragonal (*P*4/*ncc*) phase.

Table 2. *L*a*b Color Coordinates of $Ca_{1-x}Mg_xCrSi_4O_{10}$ Samples**

composition	*L**	*a**	*b**
$CaCrSi_4O_{10}$	45.73	13.45	-1.74
$Ca_{0.9}Mg_{0.1}CrSi_4O_{10}$	43.32	9.72	-1.85
$Ca_{0.8}Mg_{0.2}CrSi_4O_{10}$	42.12	9.34	-1.36
$CaCrSi_4O_{10}$-HNO_3[a]	45.60	13.44	-1.76
$CaCrSi_4O_{10}$-NaOH[a]	45.74	13.45	-1.73

[a]Data collected after stirring samples in 50% HNO_3 (aq.) or 1 M NaOH.

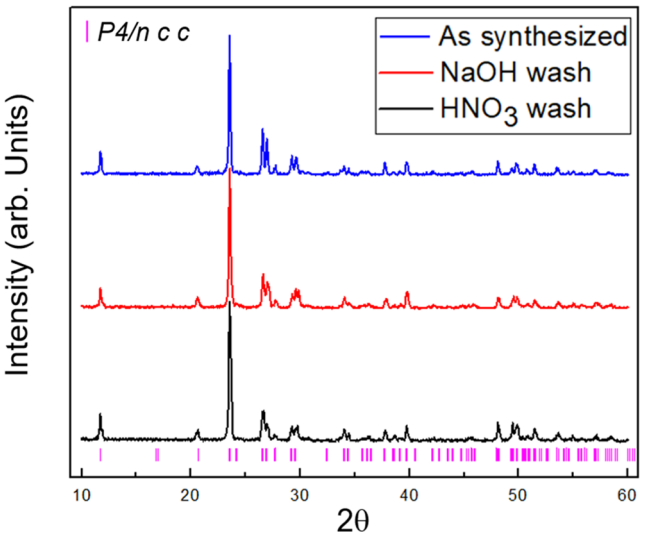

Figure 7. XRD patterns for a $CaCrSi_4O_{10}$ sample before and after acid/base tests. The vertical bars (pink) indicate the expected reflection positions for the tetragonal (*P*4/*ncc*) phase.

with other compounds in the series, all of which are durable and remain unaltered structurally and optically upon exposure to strong acids and alkalis.

The absorption spectra of $Ca_{1-x}Mg_xCrSi_4O_{10}$ (x = 0–0.2) samples show similar peaks, which may be analyzed by using group theory selection rules. The point symmetry of the crystallographic position occupied by Cr^{2+} in the $CaCrSi_4O_{10}$ structure is actually C_4. This symmetry represents the overall environment of the Cr^{2+} ion. Since the second nearest neighbors are oxygen atoms that are more than twice as far

https://doi.org/10.1021/acs.chemmater.4c00253
Chem. Mater. XXXX, XXX, XXX−XXX

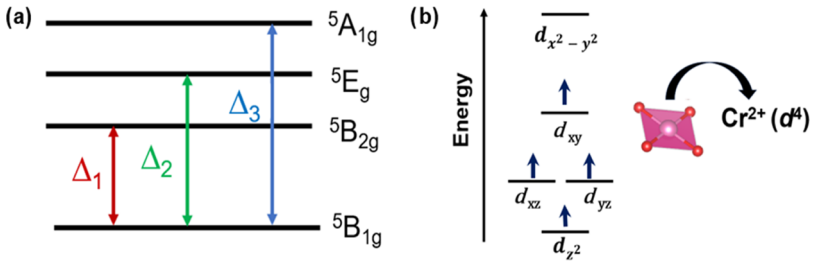

Figure 8. (a) Electronic states of Cr^{2+} in $Ca_{1-x}Mg_xCrSi_4O_{10}$ series (In D_{4h} group symmetry species of d orbitals are d_{z^2}, a_{1g}; $d_{xz,yz}$, e_g; d_{xy}, b_{2g}; $d_{x^2-y^2}$, b_{1g}). (b) Schematic energy levels for the spin-up Cr^{2+} $3d$ orbitals in the square planar coordination (D_{4h} symmetry).

from the Cr^{2+} as the four nearest neighbors, it is reasonable to consider only the planar [CrO_4] unit. The Cr^{2+} is only 0.0025 Å out of the plane of the four bonding O atoms, so it is reasonable to assume the local symmetry of Cr^{2+} is then D_{4h}.[22,29] In other words, the Cr^{2+} occupies the site with 4-fold symmetry and is in nearly ideal square planar coordination. For the D_{4h} symmetry, either the d_{z^2} orbital or the degenerate d_{xz}, d_{yz} orbitals will be at the lowest energy level because the ligand electrons are only available in the xy plane; therefore, they experience the least electrostatic repulsion. Then comes the orbitals in the xy plane, $d_{x^2-y^2}$, and d_{xy}; $d_{x^2-y^2}$ comes on top as this orbital is directed toward the ligand making them experience the highest repulsion. Thus, there can be two possible ground states, one with d_{z^2} orbital and the other with degenerate d_{xz}, d_{yz} orbitals. Burns et al.[30] proved the existence of d_{z^2} as the ground state for the gillespite mineral ($BaFeSi_4O_{10}$) with Fe^{2+} (d^6) in D_{4h} symmetry. For the weak field instance, Cr^{2+} $3d$ shell electronic structure can be considered as a single positive hole moving in the field of a spherically symmetric $3d^5$ core, similar to Cu^{2+} ($3d^9$) in $BaCuSi_4O_{10}$, analyzed as a single positive hole moving in the field of a $3d^{10}$ core.[31] In contrast, in the case of $BaFeSi_4O_{10}$ (gillespite) containing Fe^{2+} ($3d^6$), $3d$ shell electronic structure can be considered as a single d electron moving in the field of a spherically symmetrical $3d^5$ core.[31] Hence, if divalent chromium replaces divalent iron in the gillespite, the ligand-field states emerging from the ^5D term of Cr^{2+} would have the same symmetries as those acquired from the ^5D term of Fe^{2+}, but in a reverse order of energies (Figure 8a), the schematic energy level for spin-up Cr^{2+} in D_{4h} symmetry is shown in Figure 8b. The electronic state configuration of each state is listed in Table 3.

Table 3. Electronic State Configuration of Each State of Cr^{2+} in $Ca_{1-x}Mg_xCrSi_4O_{10}$ Series

states	configuration
$^5A_{1g}$	$d_{z^2}^2$, $d_{xz,\,yz}^2$, d_{xy}^1, $d_{x^2-y^2}^1$
^5E_g	$d_{z^2}^1$, $d_{xz,\,yz}^1$, d_{xy}^1, $d_{x^2-y^2}^1$
$^5B_{2g}$	$d_{z^2}^1$, $d_{xz,\,yz}^2$, d_{xy}, $d_{x^2-y^2}^1$
$^5B_{1g}$	$d_{z^2}^1$, $d_{xz,yz}^2$, d_{xy}^1, $d_{x^2-y^2}^1$

The optical absorption spectrum of $CaCrSi_4O_{10}$ powder is shown in Figure 9; the absorption peaks can be attributed to d-d transitions accompanied by vibronic coupling. According to the Laporte selection rule, d-d transitions are forbidden as they are g-g transitions.[30] However, through vibronic coupling, transitions can be allowed by simultaneous excitation of the u (odd) vibrational mode. The normal mode symmetries of the [CrO_4] unit are determined to be $A_{1g} + A_{2u} + B_{1g} + B_{2g} + B_{2u} +$

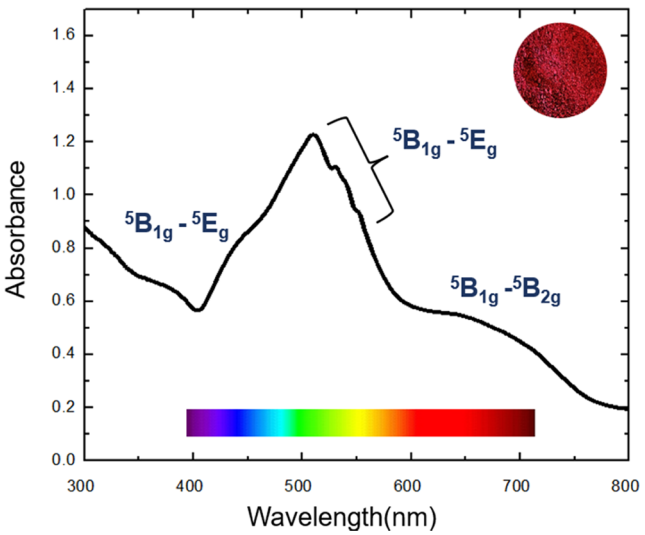

Figure 9. Optical absorption spectrum of a $CaCrSi_4O_{10}$ powder sample.

$2E_u$.[30] In Table 4, possible transitions to excited quintet states have been deduced by assuming simultaneous excitation of the normal vibration from its ground state to its first excited state. The energy ΔE_{obs} of the peak position maximum is expressed by the energy gap ΔE_e of the electronic states and the vibrational frequency ν that allows the transition by the equation $\Delta E_{obs} = \Delta E_e + h\nu$, where h is Planck's constant.

The optical absorption spectrum of the $CaCrSi_4O_{10}$ polycrystalline sample can be interpreted as an addition of the axial or σ ($\vec{E} \perp c$) spectrum, and π ($\vec{E} \parallel c$) spectrum of a single crystal,[22] suggesting grains are randomly oriented in different directions in the powder sample. The polarized spectra show only one peak in the ~670 nm region in the axial or σ ($\vec{E} \perp c$) spectrum, while its absence in the π ($\vec{E} \parallel c$) spectrum makes sense because the direct product for the $^5B_{1g} \rightarrow {}^5B_{2g}$ transition gives A_{1u}, which is not included in the normal vibrational modes for the [CrO_4] unit and therefore the transition is not allowed (Tables 4 and 5). In the axial or σ ($\vec{E} \perp c$) spectrum, three peaks (~500 nm) belong to the $^5B_{1g} \rightarrow {}^5E_g$ transition; ideally, there should be two peaks deduced from the direct product, but the interaction between these modes can occur, leading to the simultaneous occurrence of several modes, justifying the presence of three peaks (Tables 4 and 5). In the π ($\vec{E} \parallel c$) spectrum, a peak around 450 nm can be assigned to the $^5B_{1g} \rightarrow {}^5E_g$ transition accompanied by the E_u vibrational mode. A comparison of the polarized and powder spectrum peaks with the predicted transitions (Table 5) reveals that the 670 nm peak in the powder optical spectrum belongs to the $^5B_{1g} \rightarrow {}^5B_{2g}$ transition, three peaks between 510 and 550

https://doi.org/10.1021/acs.chemmater.4c00253
Chem. Mater. XXXX, XXX, XXX−XXX

Table 4. Vibronically Allowed Transitions of Cr^{2+} in $Ca_{1-x}Mg_xCrSi_4O_{10}$ Series

electric vector polarization	electric vector group theory representation (τ_μ)	transition ($\Psi_g \rightarrow \Psi_e$)	direct Product ($\tau_g * \tau_\mu * \tau_e$)	vibrational mode allowing vibronic coupling
parallel to c ($\vec{E} \parallel c$)	A_{2u}	$^5B_{1g} \rightarrow {}^5B_{2g}$	A_{1u}	*none*
		$^5B_{1g} \rightarrow {}^5E_g$	E_u	E_u
		$^5B_{1g} \rightarrow {}^5A_{1g}$	B_{2u}	B_{2u}
perpendicular to c ($\vec{E} \perp c$)	E_u	$^5B_{1g} \rightarrow {}^5B_{2g}$	E_u	E_u
		$^5B_{1g} \rightarrow {}^5E_g$	$A_{1u+}\ A_{2u+}\ B_{1u+}\ B_{2u}$	$A_{2u} + B_{2u}$
		$^5B_{1g} \rightarrow {}^5A_{1g}$	E_u	E_u

Table 5. Absorption Maxima in the Polarized and Powder Spectra of $CaCrSi_4O_{10}$

polarized spectra[a] band position (nm)	powder spectra band position (nm)	assignment (Table 4)
($\vec{E} \parallel c$) – 453	438	$^5B_{1g} \rightarrow {}^5E_g$
($\vec{E} \perp c$) – 511	511	$^5B_{1g} \rightarrow {}^5E_g$
($\vec{E} \perp c$) – 530	531	$^5B_{1g} \rightarrow {}^5E_g$
($\vec{E} \perp c$) – 551	551	$^5B_{1g} \rightarrow {}^5E_g$
($\vec{E} \perp c$) – 670	670	$^5B_{1g} \rightarrow {}^5B_{2g}$

[a]From Belsky et al.[22]

nm belong to the $^5B_{1g} \rightarrow {}^5E_g$ transition, and the peak at 438 nm also belongs to the $^5B_{1g} \rightarrow {}^5E_g$ transition, suggesting that the selection rules are consistent with the observed spectrum.

Although the observed optical spectra and the resulting intense color can be interpreted solely through vibronic coupling, it is likely that the presence of Cr^{2+} slightly away (0.0025 Å) from the center of the square planar coordination can remove the inversion center, which could relax the orbital selection rule and contribute to the enhancement of color.

Lastly, we have investigated the usefulness of $Ca_{1-x}Mg_xCrSi_4O_{10}$ magenta pigments as a near-infrared (NIR) reflective material. NIR reflectivity is a property necessary for compounds to be used as energy-saving heat reflection colorants ("cool pigments") and is the subject of increasing interest for climate change mitigation by decreasing energy use for cooling buildings, pavements, and automobiles.[32] NIR reflectance spectra (900–2000 nm) exhibit ~70% reflectance for the $Ca_{1-x}Mg_xCrSi_4O_{10}$ series (Figure 10) in the near-infrared region, categorizing these materials as potential "cool" pigments.

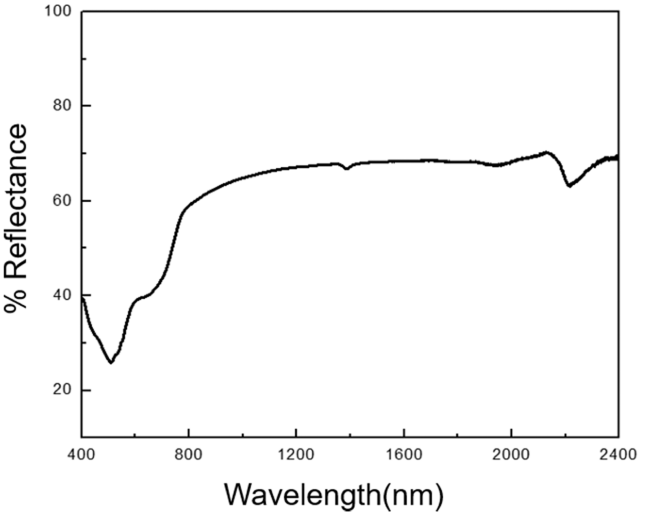

Figure 10. Near-IR spectrum of $CaCrSi_4O_{10}$.

CONCLUSIONS

Polycrystalline samples of $Ca_{1-x}Mg_xCrSi_4O_{10}$ (x = 0.0–0.2) were synthesized through two diffrent solid-state synthesis methods and characterized structurally and optically. There is a decrease in the cell edge as a function of magnesium addition. This is mainly due to the smaller size of Mg^{2+} relative to that of Ca^{2+}. Magnetic analysis of $CaCrSi_4O_{10}$ confirmed the existence of divalent chromium. Thermogravimetric analysis (TGA) of the $CaCrSi_4O_{10}$ sample showed that the compound was quite stable up to 500 °C when heated in air. The optical spectra of the series are consistent with Cr^{2+} in square planar coordination with $^5B_{1g}$ as the ground state, corresponding to the configuration, $d^1_{z^2}$, $d^2_{xz,\,yz}$, d^1_{xy}, $d^1_{x^2-y^2}$. The observed transitions can be attributed to electronic transitions from the $^5B_{1g}$ state to other quintet states of Cr^{2+}, occurring by the mechanism of *d-d* transitions accompanied by vibronic coupling. The pigments are stable in both strongly acidic and basic environments with no change in structure or color properties after treatment. The resulting samples show fairly high heat reflectance desired for cool pigment applications. This opens the field for exploring other cool, intense, and durable pigments with Cr^{2+} as a chromophore in different coordinations.

AUTHOR INFORMATION

Corresponding Author

M. A. Subramanian – *Department of Chemistry, Oregon State University, Corvallis, Oregon 97331, United States;* orcid.org/0000-0001-5487-043X; Email: mas.subramanian@oregonstate.edu

Authors

Anjali Verma – *Department of Chemistry, Oregon State University, Corvallis, Oregon 97331, United States*

Jun Li – *Department of Chemistry, Oregon State University, Corvallis, Oregon 97331, United States;* orcid.org/0000-0002-6911-4474

Complete contact information is available at: https://pubs.acs.org/10.1021/acs.chemmater.4c00253

Notes

The authors declare no competing financial interest.

ACKNOWLEDGMENTS

The work done at Oregon State University was supported by NSF Grant No. DMR-2025615. The authors thank Professor Arthur Ramirez of UC, Santa Cruz, for magnetic measurements.

REFERENCES

(1) Rao, C. N. R. Novel materials, materials design and synthetic strategies: recent advances and new directions. *J. Mater. Chem.* **1999**, *9* (1), 1−14.

(2) Subramanian, M. A.; Li, J. YInMn blue-200 Years in the making: New intense inorganic pigments based on chromophores in trigonal bipyramidal coordination. *Mater. Today Adv.* **2022**, *16*, No. 100323.

(3) Nassau, K. The origins of color in minerals. *Am. Mineral.* **1978**, *63* (3−4), 219−229.

(4) Burns, R. G. Colours of gems. *Chem. Br.* **1983**, *19* (12), 1004−1007.

(5) Nassau, K. The fifteen causes of color. In *AZimuth*; Elsevier, 1998; Vol. *1*, pp 123−168.

(6) Subramanian, M. A.; Li, J. Challenges in the rational design of intense inorganic pigments with desired colours. *Nat. Rev. Mater.* **2023**, *8* (2), 71−73.

(7) Kupferschmidt, K. In search of blue. *Science* **2019**, *364*, 424−429.

(8) Burns, R. G. *Mineralogical applications of crystal field theory*; Cambridge university press, 1993.

(9) Williams, A. F. *A theoretical approach to inorganic Chemistry*; Springer-Verlag: Berlin Heidelberg, 1979.

(10) Ball, P. *Bright earth: art and the invention of color*; University of Chicago Press, 2003.

(11) Berke, H. The invention of blue and purple pigments in ancient times. *Chem. Soc. Rev.* **2007**, *36* (1), 15−30.

(12) Pabst, A. Structures of some tetragonal sheet silicates. *Acta Crystallogr.* **1959**, *12* (10), 733−739.

(13) Jaksch, H.; Seipel, W.; Weiner, K. L.; Goresy, A. El. Egyptian blue-cuprorivaite a window to ancient Egyptian technology. *Naturwissenschaften* **1983**, *70*, 525−535.

(14) Pabst, A. Crystal structure of gillespite, $BaFeSi_4O_{10}$. *Am. Mineral.: J. Earth Planet. Mater.* **1943**, *28* (6), 372−390.

(15) Kendrick, E.; Kirk, C. J.; Dann, S. E. Structure and colour properties in the Egyptian Blue Family, $M_{1-x}M'_xCuSi_4O_{10}$, as a function of M, M′ where M, M′ = Ca, Sr and Ba. *Dyes Pigm.* **2007**, *73* (1), 13−18.

(16) Smith, A. E.; Mizoguchi, H.; Delaney, K.; Spaldin, N. A.; Sleight, A. W.; Subramanian, M. A. Mn^{3+} in trigonal bipyramidal coordination: a new blue chromophore. *J. Am. Chem. Soc.* **2009**, *131* (47), 17084−17086.

(17) Smith, A. E.; Comstock, M. C.; Subramanian, M. A. Spectral properties of the UV absorbing and near-IR reflecting blue pigment, $YIn_{1-x}Mn_xO_3$. *Dyes Pigm.* **2016**, *133*, 214−221.

(18) Haggerty, S. E.; Boyd, F. R.; Bell, P. M.; Finger, L. W.; Bryan, W. B. Opaque minerals and olivine in lavas and breccias from Mare Tranquillitatis. In *Geochimica et Cosmochimica Acta Supplement, Vol. 1. Proceedings of the Apollo 11 Lunar Science Conference held 5−8 January, 1970 in Houston, TX.Vol. 1: Mineraolgy and Petrology*; Levinson, A. A., Ed.; Pergammon Press: New York, 1970; Vol. *1*, p 513.

(19) Steele, I. M. Lunar mineralogy. In *Mineralogy, Encyclopedia of Earth Science*; Springer: Boston, MA, 1981; pp 217−225.

(20) Meyer, H. O. A.; Boyd, F. R. Composition and origin of crystalline inclusions in natural diamonds. *Geochim. Cosmochim. Acta* **1972**, *36* (11), 1255−1273.

(21) Gasparik, T. Some Phase Relations Involving Chromous Pyroxenes and Other Cr^{2+} Bearing Phases at Pressures Less than 1 atm. In *LUNAR AND PLANETARY SCIENCE XII, P. 333−335. Abstract.*, 1981; Vol. *12*, pp 333−335.

(22) Belsky, H. L.; Rossman, G. R.; Prewitt, C. T.; Gasparik, T. Crystal structure and optical spectroscopy (300 to 2200 nm) of $CaCrSi_4O_{10}$. *Am. Mineral.* **1984**, *69* (7−8), 771−776.

(23) Miletich, R.; Allan, D. R.; Angel, R. J. The synthetic Cr^{2+} silicates $BaCrSi_4O_{10}$ and $SrCrSi_4O_{10}$: The missing links in the gillespite-type $ABSi_4O_{10}$ series. *Am. Mineral.* **1997**, *82* (7−8), 697−707.

(24) Shannon, R. D. Revised effective ionic radii and systematic studies of interatomic distances in halides and chalcogenides. *Acta Crystallogr., Sect. A: Cryst. Phys., Diffr., Theor. Gen. Crystallogr.* **1976**, *32* (5), 751−767.

(25) Bain, G. A.; Berry, J. F. Diamagnetic corrections and Pascal's constants. *J. Chem. Educ.* **2008**, *85* (4), 532.

(26) Konica Minolta, I. *Precise Color Communication* Konica Minolta, Inc.2011−2019 https://www.konicaminolta.com/instruments/knowledge/color/part1/07.html.

(27) Li, J.; Lorger, S.; Stalick, J. K.; Sleight, A. W.; Subramanian, M. A. From serendipity to rational design: tuning the blue trigonal bipyramidal Mn^{3+} chromophore to violet and purple through application of chemical pressure. *Inorg. Chem.* **2016**, *55* (19), 9798−9804.

(28) Li, J.; Subramanian, M. A. Inorganic pigments with transition metal chromophores at trigonal bipyramidal coordination: Y(In,Mn)-O_3 blues and beyond. *J. Solid State Chem.* **2019**, *272*, 9−20.

(29) Cotton, F. A. *Chemical applications of group theory*; John Wiley & Sons, 1991.

(30) Burns, R. G.; Clark, M. G.; Stone, A. J. Vibronic polarization in the electronic spectra of gillespite, a mineral containing iron (II) in square-planar coordination. *Inorg. Chem.* **1966**, *5* (7), 1268−1272.

(31) Clark, M. G.; Burns, R. G. Electronic spectra of Cu^{2+} and Fe^{2+} square planar co-ordinated by oxygen in $BaXSi_4O_{10}$. *J. Chem. Soc. A* **1967**, 1034−1038.

(32) Jose, S.; Joshy, D.; Narendranath, S. B.; Periyat, P. Recent advances in infrared reflective inorganic pigments. *Sol. Energy Mater. Sol. Cells* **2019**, *194*, 7−27.

https://doi.org/10.1021/acs.chemmater.4c00253
Chem. Mater. XXXX, XXX, XXX−XXX